Reducing uncertainty of karst aquifer modeling with complementary hydrological observations for the sustainable management of groundwater resources

Yohann Cousquer, Hervé Jourde

Reducing Uncertainty of Karst Aquifer Modeling with Complementary Hydrological Observations for the Sustainable Management of Groundwater Resources

Yohann Cousquer[1], Herve Jourde[1]

1 HSM, Univ. Montpellier, CNRS, IMT, IRD, Montpellier, France

Abstract

A quantitative estimation of the sustainability of groundwater resources is a challenge for water supply in most regions of the world. Sustainability can be estimated through numerical simulation, but uncertainty of models somehow limits the reliability of models' predictions. To overcome this limitation, we explore how parametric and predictive uncertainties is reduced by adding complementary groundwater and surface water dynamics data to a lumped parameter model. This is illustrated with the example of a Mediterranean karst hydrosystem pumped at high flow rate (~ 1 m^3 s^{-1}) to supply water to about 350,000 habitants. A lumped parameter model was set up to simulate spring discharge, water table levels and surface water discharge measured within this karst hydrosystem over a 40 year period. Then, a parameter estimation and uncertainty quantification, based on groundwater discharge, water table levels and surface water discharge observations, was conducted with a Bayesian approach. Our study illustrates how the consideration of complementary hydrological data allows reducing parametric and predictive uncertainty and improving model performance. The model is then applied to assess the impact of an increasing groundwater abstraction according to different prospective scenarios, with a focus on the storage and dynamic of flux between the different compartments of the karst hydrosystem. Based on simulation results and related predictive uncertainty, a groundwater abstraction threshold, which must not be exceeded for a sustainable management of the groundwater resource, is determined.

1. Introduction

With the increasing water supply, the need for karst groundwater has grown, in particular in the Mediterranean area (Sivelle et al., 2021). In this context, understanding and predicting the influence of increased groundwater abstraction on the functioning and storage of karst hydrosystem is an important issue.

In order to correctly describe and predict karst hydrosystem behavior at catchment scale, groundwater (GW) and surface water (SW) must be considered as a same entity, and thus as a unique water resource (Winter et al., 1999; Sophocleous, 2002; Bailly-Comte et al., 2009). Indeed, intensive water abstraction and/or contamination of groundwater is likely to affect surface water, and inversely, because of their high interaction and interrelationship (Bailly-Comte et al., 2009). During extreme events, the addition of both karst groundwater and surface water discharge can also be at the origin of floods and flashfloods (e.g., López-Chicano et al., 2002; Pinault et al., 2005; Bonacci et al., 2006; Najib et al., 2008; Naughton et al., 2012; Jourde et al., 2014). These interactions and relationships between GW and SW have been studied mainly over short time scales (flood event scale) with the help of hydrodynamic time series analysis or hydrological modeling (i.e., Jourde et al. 2007, Bailly-Comte et al., 2009; Bailly-Comte et al., 2012, Darras et al., 2017).

Due to the heterogenous nature of karst aquifers, distributed modeling cannot be easily implemented and calibrated because of difficulties in obtaining the necessary input data (Hartmann et al., 2014). Furthermore, times series generally consist in discharge measurements at the main outlets of the catchment. For this reason, modeling the hydrodynamics of such complex karst systems generally consists in the simulation of rainfall-discharge relationship with lumped parameter models (Bittner et al., 2018; Dubois et al., 2020; Labat et al., 1999; Ladouche et al., 2014; Long & Derickson, 1999, Mazzilli et al., 2011). Modeling can further be used to describe the global responses of a karst system to either climatic or anthropogenic forcing, in terms of water table or spring discharge fluctuations (Sivelle et al, 2021). Indeed, it may be of major importance to assess the consequences of intensive groundwater exploitation, especially in Mediterranean region (Vallejos et al., 2015) However, parameters involved in hydrological models are generally obtained by history-matching against observations such as spring discharge and sometimes water table level.

The invers problem in hydrology is generally ill-posed because the solution does not exist uniquely and model output varies non-continuously as the unput data changes smoothly (Anderman and Hill, 1997; Carrera et al., 2005; Zhou et al. 2014), which may lead to non-uniqueness, non-existence and non-steadiness of the solution (Zhou et al. 2014). In this case, an infinite number of parameter sets can calibrate the model equally well. To overcome this issue, some improvements of inversion tools and parameters dimension reduction have been developed. For example, the active subspace method was recently proposed to reduce the dimension of complex hydrological models (Bittner et al., 2020; Teixeira et al., 2019). The use of multi objective calibration framework have also been extended by considering autocorrelation of the discharge time series in addition to the classical least mean square errors (Moussu et al., 2011). The use of additional observations, such as water quality data (Hartmann et al 2017); electrical conductivity (Chang et al., 2021) or stream-aquifer mixing ratio (Cousquer et al., 2018)., alleviate the ill-posedness of the inverse problem and lead to a more robust model and a reduction of parametric uncertainty.

In this study, we propose to quantify both parametric and predictive uncertainty reduction of a lumped parameter model used for the hydrological modelling of a karst hydrosystems. This model, designed with the KarstMod modelling platform (Mazzilli et al., 2019), allows accounting for different reservoirs representative of distinct karst compartments (epikarst, matrix, conduit).

To reduce uncertainty, we consider an additional independent hydrological observation in complement to spring discharge and water table level, i.e, the outflow from the epikarstic compartment, in the parameter estimation procedure realized with a Bayesian approach. This multi objective calibration improves the robustness of the model by reducing uncertainty. The model is used afterward to assess an abstraction flow rate threshold and estimate a sustainable management based on several water resource management scenarios.

The paper is organized as follows. In Section 2, we describe the Lez Mediterranean karst system and the groundwater management of the aquifer, as well as the data considered in this study. In Section 3, we present the structure of the lumped parameter model used to simulate karst spring discharge, the parameter estimation procedure, and the methodology adopted to assess the influence of various management options on the functioning of the karst hydrosystem. Section 4 is devoted to the analysis of the changes in the parametric

uncertainty when complementary observation data (water table data and surface discharge observation) are added to the objective function; then we discuss the consequences of various groundwater abstraction scenarios on the groundwater resource, internal fluxes between compartments of the karst hydrodystem and discharge at the karst spring.

Based on simulation results and related predictive uncertainty, a groundwater abstraction threshold that must not be exceeded for a sustainable management of the groundwater resource, is finally determined. Section 5 presents the conclusions.

2. Study Site: The Lez Karst Hydrosystem

The Mediterranean karst hydrosystem considered in this study is located in the South of France and is encompassed between the Hercynian basement of the Cévennes to the north and the Mediterranean Sea to the south.

With a main spring called Lez Spring, the karst aquifer supplies water to the city of Montpellier, southern France, since the end of the XIXth century. Nowadays, these are about 10 000 m^3 day^{-1} of drinking water which are provided to about 350 000 habitants of the metropolitan area of Montpellier city. The particularity of this aquifer lies in the management of the water resource, which consists in pumping groundwater directly within the karst conduit at a higher rate (~1000 l s^{-1}) than the low-water spring discharge (~370 l s^{-1}, Jourde et al., 2011). This management, referred to as “active management”, allows to extract part of the stored and naturally renewable groundwater but generates large drawdown (~ 25 m below the overflow level of the karst spring) during low-flow periods.

The recharge area of the Lez Spring catchment is estimated to be about 150 km^2, corresponding mostly to the surface area where the aquifer limestone directly outcrops (Mazzilli, 2011). The exact area of the aquifer that feeds the Lez Spring, referred to as the hydrogeological basin (Fig. 1), is not precisely known but is estimated to be around 250 km^2 (Leonardi et al., 2011). The intense Mediterranean events in autumn are the main contributors to the annual recharge. Annual rainfall occurs principally from September to December and to a lesser extent from March to May (Dausse et al., 2019). The mean annual precipitation ranges from about 600 mm to more than 1500 mm.

The Lez aquifer is mainly composed of Upper Jurassic and Early Cretaceous limestone. The aquifer is overlain by the Lower Jurrassic marls and is locally covered by a succession of Early

Cretaceous marls and marly limestone. The aquifer shows a high degree of karstification developed from the Middle Cretaceous to the current period (Leonardi et al., 2011). The deep karstification at the origin of karst conduits and channels at depth is attributed to the Messinian Salinity Crisis (about 5.5 My ago) when the Mediterranean Sea-level dropped about 1500 m due to the closing of the Gibraltar straights (Audra et al., 2004; Clauzon et al., 2005). The aquifer is divided into several NE-SW normal faults related to the Pyrenean orogeny (Eocene) and later impacted by the Oligocene extension phase (Seranne et al., 1995; Benedicto et al., 1999).

The Lez Spring, which was a perennial spring under natural conditions (before high flow rate pumping), feeds the Lez River. Besides this river, the Terrieu and the Lirou intermittent streams drain the upper part of the karst system and flow across the hydrosystem, mainly during intense rainfall events. The hydrogeological karst catchment encompasses the hydrological basin of the Lez River at the entrance of Montpellier (Lavalette gauging station), the area of which being about 130 km^2 (Fig. 1).

2.1. Observations

2.1.1. Discharge data and water table measurements at the Lez Spring

We considered discharge and water table time series at the Lez Spring, as well as discharge of the Lez River at the Lavalette Gauging Station (Fig. 1) over the 1982-2020 period. Discharge measured at the Lavalette Gauging Station corresponds to discharge at the outlet of the hydrological watershed that drains the Lez River and its main tributaries (Lirou and Terrieu streams) which flow essentially after intense Mediterranean rainfall events. Then, surface flow composed of secondary outflows of epikarstic intermittent springs from the karst aquifer can be estimated as follows:

$$Q_{surface} = Q_{Lavalette} - Q_{Lez}$$

Where $Q_{surface}$ [L^3 T^{-1}] is the estimated discharge of the secondary outlets (i.e., contribution of karst overflow through the Lirou and Terrieu streams), $Q_{lavalette}$ [L^3 T^{-1}] is the Lez River discharge recorded at the Lavalette Gauging Station (Fig. 1) and Q_{lez} [L^3 T^{-1}] is the Lez spring discharge (Fig. 1).

2.1.2. Meteorological Observations

Precipitations has been recorded with rain gauges at 4 stations located over the Lez Hydrosystem or in its surrounding (Fig. 1). Global rainfall over the recharge area, where Jurrasic and Cretaceous karst limestone formations overly, was interpolated with Thiessen polygons. Due to some gaps in precipitation time series at various of these monitoring stations, the weight of each station has been calculated over time to suit data availability.

Effective evaporation (ET) has been measured with a Flux tower in P4 (Fig. 1) at the CEFE experimental station of Puechabon (Limousin et al, 2009), build over *Quercus ilex* forest with a shallow soil characteristic of Jurassic limestone epikarst, which comprises a high proportion of stone and rocks in the top layers (75%). Maximum available water content is around 120 mm (Olioso et al., 2019) and mean annual evapotranspiration corresponds to 44% of precipitation with a high inter-annual variability depending on precipitation distribution (Limousin et al, 2009). At this site, the geology and the vegetation are like the one over the Lez Spring recharge catchment. As this experimental station is located about 13 km from the hydrogeological basin boundary and spatial variation of ET in this area is very low compared to its daily variation (Limousin et al., 2009), we considered that measurements at this site provide a good proxy of ET over the Lez spring karst catchment.

2.2 Groundwater Management of the Lez Karst Aquifer

The Lez Spring has supplied drinking water to Montpellier city and its surroundings since 1854. Initially, only part of the natural discharge of the spring was used, with an abstraction flow rate that was about 0.4 $m^3 s^{-1}$ due to the geometrical properties (diameter and slope) of the tapping conduit located at about 65 m A.S.L, one meter below the overflow level of the spring. From 1968 to 1982 water was extracted by pumping directly within the spring pool with a flow rate up to about 0.8 $m^3 s^{-1}$, which generated a water table decrease to -6.50 m below the overflow level of the spring during low flow conditions. During this period the pumping rate was sufficient to satisfy water needs, except during low flow conditions (June, July, August, and September). To overcome this issue, 4 boreholes were drilled in 1982, 400 m upstream from the Lez Spring, to intercept the main karst conduit that feeds this spring. Groundwater is currently tapped by three pumping units located at 45 m below the overflow

level of the spring and consists of two submerged pumps, connected in series and operating at variable speed with an output flowrate of 600 to 1 000 l s^{-1}, the mean pumping rate being of about 1.08 m^3 s^{-1} over the 1982-2021 period. The active management performed since 1982 allows providing a minimum discharge rate to the Lez River for ecological purposes (160 l s^{-1}, then 230 l.s^{-1} after 2018) but also satisfying the increase of water need during the dry months (Fig. 2).

3. Methods

The data used in the model were precipitation, obtained by interpolation from Thiessen method from 4 stations presented Fig. 1, effective evaporation (ET) measured at the CEFE experimental station of Puechabon (P4, Fig. 1), water table level, pumping flow rate and discharge measured at the Lez Spring, as well as surface discharge (Qs) measured at Lavalette station at daily resolution from 01.01.1982 to 12.31.2020. We set up a warm-up period from 01.01.1982 to 12.31.1986 to avoid the influence of initial condition on both model calibration and validation. So that the model appropriately captures the hydrological variability of the karst hydrosystem, the calibration period is set up from 01.01.1996 to 12.31.2005, which corresponds to a period of highly contrasted hydrometeorological conditions. The validation period covers both the (01.01.1987-12.31.1995) and the (01.01.2006-12.31.2020) periods.

3.1. Model Development and Structure

Several numerical models have already been developed to study the Lez aquifer's hydrodynamics with a view to groundwater exploitation reservoirs (Guilbot, 1975; Thiery et al., 1983; Fleury et al., 2008, Mazzili, 2011) or to simulate several scenarios of pumping under present and future climatic conditions (Marechal et al., 2018). However, the studies did not consider surface water discharge from secondary outlets and intermittent springs in the modeling. Water table levels and discharge at the Lez Spring were simulated with the KarstMod modeling platform (Mazzilli et al., 2017) which is a conceptual reservoir model dedicated to karst flow simulation. This code is a modular bucket-style conceptual model, where water fluxes cross interconnected reservoirs to quantify them over chosen time steps.

The structure of the lumped reservoir model (Fig. 2) used to simulate discharge and hydrodynamics at the Lez Spring comprises three reservoirs that can be considered as representative of different hydrological compartments. This configuration was chosen to consider the behavior of epikarst, matrix and conduit, i.e., the epikarst compartment (E), the matrix compartment (M) and the karst conduits compartment (C). Q_{loss} corresponds to the surface discharge from the epikarst compartment. Q_{pump} represents the pumping discharge from karst conduits compartment C where water table level Z is estimated from water level in C . Q_s corresponds to spring discharge. Each reservoir dynamic is driven by mass-balance equations provided by Mazzilli et al. (2017) and detailed in appendix.

3.2. Parameter Estimation

In hydrogeology, most models are mathematically ill-posed because the solution does not exist uniquely and model output varies non-continuously as the input data changes smoothly, which means that there are issues for uniqueness, identifiability, and stability of the problem solution (Ebel et al 2007, Zhou et al. 2014). To tend toward a well-posed problem, one can use various data types to constrain model solutions with a mathematical parameter space exploration. We propose to accomplish this through a stochastic approach based on Bayesian assumption with a sufficiently large prior range of parameters.

The model contains fourteen parameters to be estimated (Table 1). The parameter estimation method considered to explore parameter space to reduce the gap between observed and simulated variables (spring discharge, water table level and surface water discharge) has been developed under a R script. First, the variance based Sobol sensitivity indexes (Sobol et al. 2001; Saltelli et al. 2004) are calculated for each parameter, following the Sobol procedure (Saltelli, 2002). These sensitivity indexes are related to the decomposition of the variance of model output into terms that are due either to each parameter *i* taken singularly (first order indexes) or to interactions between parameters (global sensitivity index). The sensitivity of each parameter is described by the first order sensitivity index, which is the contribution of a single model parameter to the model output variance (Sobol et al. 2001). The sensitivity index has been calculated for a number of 10^5 parameter sets. This procedure allows identifying parameters that have a low effect on solution. A sensitivity threshold of 0.001 have been selected in order to set a fixed value for

parameters that have a very low sensitivity on the model. Following this procedure, M_0 and C_0 parameter have been set (Table 1). Other fixed parameter values (R_A and Z_0) have been chosen on expert knowledges based on field measurements. The reduction of the number of parameters to be estimated allows limiting the non-uniqueness of the solution by diminishing both over-parametrization and dimension of the parameter space.

Range of parameters have been chosen sufficiently large to properly cover the solution space.

Monte-Carlo procedure, with a latin hypercube uniform sampling of the parameter space has been set sufficiently large to explore parameter space. A sampling size of 5×10^5 parameter set has been generated. Parameter estimation is then performed based on an objective function ϕ which account for three distinct Nash Sutcliff Efficiency (NSE) values related to either spring discharge, water table level or surface water discharge:

$$\phi = \sum_{l=1}^{M} \sum_{k=1}^{K_l} \sum_{i=1}^{N_{k,l}} (\omega_{k,l} \times 1 - \frac{\sum (r_{k,l})^2}{\sum \left(obs - \overline{obs} \right)^2_{k,l}} \quad)$$

where $r_{k,l}$ is the residual value between simulation and observation, L is the number of data types (spring discharge, water table level and surface water discharge), K_l is the number of observation points for the i-th data type (1 in this case), and $N_{k,l}$ is the number of observation records for the k-th observation point of the l-th data type ($N_{k,l}$ = 1 when considering steady state values). The weighing factor of each observation is 1/M. Every observation of each data type is then well balanced in the pre-calibration objective function. In the remaining of the paper, the objective function considering spring discharge only will be referred to as $\phi tot = 1 \times \phi Q_{GW}$, the objective function considering spring discharge and water table level as $\phi tot = 0.5 \times \phi Q_{GW} + 0.5 \times \phi Q_Z$ and the objective function considering spring discharge, water table level and surface discharge as $\phi tot = 1/3 \times \phi Q_{GW} + 1/3 \times \phi Q_Z + 1/3 \times \phi Q_{SW.}$

Third, each parameter set that equally calibrates the model with a minimum value of the objective function ϕ of 0.6 is collected.

3.3 Investigating future Groundwater Management Scenarios

289 Different management scenarios have been simulated accounting for the posterior
290 parameters set that equally calibrate the model. These simulations permitted to assess the
291 effects of various management options (distinct pumping flowrate) on the functioning of the
292 karst hydrosystem under the current climate condition (similar *P* and *ET*). We estimated the
293 mean annual discharge and water table at the Lez Spring, as well as the mean annual surface
294 discharge versus the annual groundwater abstraction. This has been performed while
295 considering an increase in pumping flowrate with an increment of 0.1 $m^3 s^{-1}$, from 0 to 2 m^3
296 s^{-1}, over the same period as the calibration period (1996-2005), in order to consider highly
297 contrasted hydrometeorological conditions. Predictive uncertainty was estimated from the
298 simulations distribution that encompass all posterior parameter sets satisfying the objective
299 function.
300 Such hydrological modeling of alternative management scenarios can help us to assess the
301 tipping point between sustainable and unsustainable groundwater management, and
302 therefore the corresponding pumping flowrate that must not be exceeded.
303
304
305 **4. Results and discussion**
306 We present results of the parameter estimation procedure and uncertainty analysis, then
307 analyze the hydrological response of the hydrosystem to various groundwater withdrawal
308 scenarios.
309 Observed, simulated and associated uncertainty in the calibration period are presented in
310 Fig. 3, for spring discharge, water table level and surface discharge.
311 Table 2 shows the number of posterior parameters set that satisfied the objective function
312 threshold of 0.6 and the best objective function obtained as a function of observation
313 variables considered for parameter estimation. We can observe that, when the objective
314 function is enriched with a new type of data, the number of parameters sets satisfying the ϕ
315 threshold of 0.6 decreases and the best value of the objective function ϕ (NSE in this case)
316 also decreases both for calibration and validation period, it allows to gain in stability of the
317 results and to minimize the problem of over-fitting
318 Adding surface water discharge observations to the parameter estimation process allows to
319 improve equifinality issue by reducing the number of parameter sets that equally calibrate
320 the model, and thus the parametric uncertainty. The number of parameter sets decreases

from 6424 when accounting for spring discharge Q_s only, to 52 when accounting also for both water table levels at the spring and surface discharge (Table 1). In this way, we reduce parameters set that equally satisfied the objectif function from 1.3% to 0.01% over the 5×10^5 tested parameter sets. Reducing equifinality issues and parametric uncertainty constitute an important preliminary step to improve the confidence in model results before studying alternative management scenarios and their consequences on the sustainability of groundwater resources.

Influence of observation type posterior parameter density are presented Fig. 4. When the objective function accounts for both the discharge and the water table level, there are very few improvements in parameter uncertainty (Fig. 4), except for the estimation of compartment *C* porosity parameter (ω_c). On the contrary, when the objective function accounts for the discharge and water table level at the spring but also for the surface discharge observation, uncertainty is notably reduced for almost all parameters (Fig. 4), especially those which control surface water discharge (k_{loss}, E_{min}) and fluxes between various hydrological compartments, i.e. the epikarst compartment, the matrix compartment and the karst conduit compartment (K_{EM}, $a\mathrm{EM}$, K_{MC}, aEC, aMC).

Results of the simulations for prospective pumping scenarios (Fig. 5) indicate that the mean annual discharge linearly decreases as a function of the pumping flowrate and becomes null when the pumping flowrate reaches the mean inter-annual spring discharge of 2 $m^3\ s^{-1}$. Theoretically, pumping flowrate should be sustainable until the groundwater abstraction reaches this mean annual discharge value.

However, when we analyze the mean annual water table in the karst conduit compartment (Fig. 5), it decreases slowly and drops abruptly when the mean annual pumping rate reaches about 1.5 $m^3\ s^{-1}$ to 1.7 $m^3\ s^{-1}$ depending on predictive uncertainty, which correspond to a water table level of about 45 to 55 m a.s.l which is 10 to 20 m under spring level. Beyond this value, the table level drops indicate that the recharge is no longer sufficient to recover the spring water table level, which can lead to several years without flow at the spring and a water table level far under the current pump level.

Mean matrix to conduit flow decreases from the very beginning of pumping, and further decreases when the pumping flowrate reaches the threshold which is between 1.5 $m^3\ s^{-1}$ to 1.7 $m^3\ s^{-1}$, which contributes to the water level drop in the conduit compartment (Figure 5). A median water table level of about 50 m a.s.l correspond to a pumping flow rate value

around 1.6 m^3 s^{-1} can thus be considered as a tipping point (Gobble, 2020) indicating the change from a sustainable to an unsustainable management of the groundwater resource.

Predictive uncertainty is then evaluated for each objective function, to estimate the reliability of the prediction and to quantify the interest off adding water table level and surface discharge observations to the parameter estimation step (Figure 6). Predictive uncertainty has been quantified by using every estimated parameter set for each objective function. Predictive uncertainty was estimated by a density function considering all parameter sets satisfying the objective function. This allowed to consider the uncertainty associated to the predictive simulation under alternative management scenarios for each objective function. This uncertainty is particularly significant for values of mean annual pumping discharge around and higher than the threshold range of 1.5 m^3 s^{-1} to 1.7 m^3 s^{-1}, which defines the tipping point and corresponds to a median water table level of 50 m a.s.l. However, the mean annual pumping discharge distribution are noticeably different when considering each of the 3 objectives function Φtot, for a tipping point occurring for a selected water table level of 50 m a.s.l. The median tipping point pumping discharge value is of 1.71, 1.66 and 1.69 m^2 s^{-1} for objective function with Q_{GW}, Q_{GW} + ΦQ_Z and Q_{GW} + ΦQ_Z + ΦQ_{SW} respectively with a standard deviation for those distribution of 0.083, 0.05 and 0.033 m^2 s^{-1}. These distributions show that the uncertainty on pumping discharges associated to this tipping point is also reduced when the objective function includes complementary data, i.e water table level alone, or both water table level and surface discharge observation (Figure 6).

The median value of these distributions, and especially the distribution obtained when the objective function $\Phi tot = 1/3 \times \Phi QGW + 1/3 \times \Phi QZ + 1/3 \times \Phi QSW$ is considered in the calibration, give a better estimate of the pumping flow rate threshold, which defines the tipping point.

One limitation of the proposed method is that, beyond the tipping point pumping flowrate threshold, the quantified predictive uncertainty increases (Fig. 6). This can be explained by a lack of observations at higher pumping flowrate than the mean pumping flowrate in the parameter estimation. However, even though the uncertainty is high, this unsustainable management would generate water table levels much lower (down to 150 m drawdowns) than the spring overflow level, when groundwater abstraction discharge changes from 1.6 m^3 s^{-1} to 2 m^3 s^{-1}. In this case, the spring will be dry most of the time as the occurrence of no

flow at the Lez spring would increase from 80 to 100% when pumping flow rate changes from 1.6 $m^3 s^{-1}$ to 2 $m^3 s^{-1}$.

To further understand the change in hydrosystem dynamics under such anthropogenic forcing, we performed simulations considering i) the mean annual pumping rate of 1 $m^3 s^{-1}$ which corresponds to the current management scheme over the 1982-2020 period, then a groundwater abstraction ii) slightly below (1.5 $m^3 s^{-1}$) and iii) above (1.7 $m^3 s^{-1}$) the pumping flow rate threshold.

When pumping flowrate overpasses 1.6 $m^3 s^{-1}$ threshold, the water table level remains below the overflow level of the springover a very large period (spring discharge is null). In this case, pumped groundwater comes from water stored in the aquifer during wet years (i.e., 1987, 1995, 1996, cf red boxes Fig. 7).

Under the current management with a groundwater abstraction of about 1 $m^3 s^{-1}$, we can observe an overflow at the spring 48% of the time. For a pumping flowrate of 1.5 $m^3 s^{-1}$, spring flows 28% of the time, and 18% of the time when the pumping flowrate reaches 1.7 $m^3 s^{-1}$. Under the current management, aquifer recharge is thus sufficient to provide water at the spring every year but becomes insufficient when the pumping flowrate overpasses 1.6 $m^3 s^{-1}$. For example, there are four complete years (over 9 years) with no flow at the spring for a pumping flowrate of 1.7 $m^3 s^{-1}$ (Fig. 7).

Furthermore, when groundwater abstraction overpasses the 1.6 $m^3 s^{-1}$ threshold, there is a drastic drop of the water table level much below the authorized drawdown (30 m), which corresponds to a piezometry of 35 m. For greater drawdowns such as the one observed when the pumping flowrate reaches 1.7 $m^3 s^{-1}$ (> 50 m), the hydrodynamic response of the aquifer is unknown and the expected recovery during wet years might be altered.

5. Summary and Conclusion

418 The presented case study shows how the use of complementary hydrological data from
419 different compartments of a karst hydrosystem allows improving the performance of karst
420 hydrological modelling, and noticeably reducing both parametric and predictive
421 uncertainties.
422 The proposed karst hydrological model simulates spring discharge, water table levels and
423 surface discharge. These complementary hydrological data are considered for model
424 performance estimate on the basis of distinct objective functions. The parameter estimation
425 is performed with a Bayesian procedure based on a Monte-Carlo approach considering
426 objectives functions that contain these complementary hydrological data. When surface
427 water discharge observations as well as water table levels and discharge observations at the
428 spring are considered in the objective function, both parametric and predictive uncertainties
429 are greatly reduced.
430 This study also gives insights about the hydrological response of a karst hydrosystem under
431 high anthropogenic pressure (increased groundwater abstraction). By analyzing the
432 hydrodynamic response to various management options under current climate conditions, a
433 groundwater abstraction threshold (maximum pumping flow rate) that must not be
434 overpassed for a sustainable management of the groundwater resource has been identified.
435 This pumping flow rate value can be considered as a tipping point in the functioning of the
436 karst aquifer with unknown consequences on the recovery of the aquifer after successive
437 dry years or droughts. Indeed, we would expect that pumping flowrate corresponding to the
438 mean interannual outflow at the spring (2 $m^3 s^{-1}$) should be possible. However, the
439 prediction of water table levels and spring discharge shows that recharge is insufficient to
440 recover annual water depletion each year when the pumping flowrate rate exceeds about
441 1.6 $m^3 s^{-1}$. Beyond this pumping flowrate threshold, no flow at the spring would be observed
442 44% of the time, and the occurrence of such events would increase significantly for higher
443 pumping flowrate. Given these results and due to the variability of hydroclimatic conditions
444 that limits the recharge of the aquifer during some years, a sustainable management of the
445 groundwater resource will be possible only if the pumping flowrate remains below the
446 pumping flowrate threshold of 1.6-1.7 $m^3 s^{-1}$ evidenced in this study.
447 It thus points out the risk of unsustainability of the water resource management, especially
448 in case of recurrent dry years. This disequilibrium might not only endanger the water supply,
449 but also the downstream groundwater dependent ecosystem. The proposed methodology,

which allows reducing hydrologic modeling uncertainty and thus improving simulations results, should help stakeholders to take the right decisions for a sustainable management of the karst groundwater resource.

Acknowledgments

The authors would like to thank the French Karst National Observatory Service (SNO KARST) initiative at the INSU/CNRS which aims to strengthen the dissemination of knowledge and promotes crossdisciplinary research on karst systems at the national scale, for their support on the use of the KarstMod model. The authors are grateful to the editor and the two anonymous reviewers for their valuable comments.

Appendix

Each reservoir dynamic is driven by mass-balance equations provided by Mazzilli et al. (2017), is here detailed:

$$\frac{dE}{dt} = P - ET - Q_{EM} - Q_{EC}$$

$$\frac{dM}{dt} = Q_{EM} - Q_{MC}$$

$$\frac{dC}{dt} = Q_{EC} - Q_{CS}$$

Where:

$$Q_{EM} = (k_{EM} \times E\ )^{aEM} if E\ > E_0, otherwise Q_{EM} = 0$$

$$Q_{EC} = (k_{EC} \times E\ )^{aEC} if E\ > E_0, otherwise Q_{EC} = 0$$

$$Q_{MC} = k_{MC} \times (M - C)$$

$$Q_{loss} = (k_{loss} \times E_{loss}\ )^{aloss} if E\ > E_{loss}, otherwise Q_{loss} = 0$$

$$Q_{CS} = (k_{CS} \times C)^{aCS}$$

where P and ET are respectively rainfall and evapotranspiration [L], *E*, *M* and *C* are respectively the water levels in the reservoirs E, M and C, k is the recession coefficient associated to the flow from reservoir E, M, or C to reservoir M, C or to the outlet S and Q is the discharge from reservoir E, M, or C to reservoir M, C [L/T]. Discharge [L^3/T] is computed by the product of Q with the total surface of the recharge area (RA).

Q_{loss} corresponds to the discharge from the epikarst compartment E, when the E level becomes higher than E_{loss}. This discharge can be considered as representative of the surface discharge from the Lirou and Terrieu intermittent streams which flow when the water level in the epikarst is sufficiently high. Z corresponds to the water level in reservoir C [L], and its dynamic can be considered as representative of the water table level changes observed in the main karst conduit that feeds the Lez Spring. The water table level is obtained as follows:

$$Z = Z_0 + \frac{C}{\omega}$$

where Z_0 [L] corresponds to an overflow threshold (which is similar to the overflow level at the karst spring) and ω [-] to the effective porosity.

References:

Anderman, E. R., & Hill, M. C. (1997). *ADVective-transport Obeservation (ADV) Package, a Computer Program for Adding Advective-transport Observations of Steady-state Flow Fields to the Three-dimensional Ground-water Flow Parameter-estimation Model MODFLOWP*. US Geological Survey.

Aster, R. C., Borchers, B., & Thurber, C. H. (2018). *Parameter estimation and inverse problems*. Elsevier.

Audra, P., Mocochain, L., Camus, H., Gilli, É., Clauzon, G., & Bigot, J. Y. (2004). The effect of the Messinian Deep Stage on karst development around the Mediterranean Sea. Examples from Southern France. Geodinamica Acta, 17(6), 389-400.

Bailly-Comte, V., Jourde, H., & Pistre, S. (2009). Conceptualization and classification of groundwater–surface water hydrodynamic interactions in karst watersheds: Case of the karst watershed of the Coulazou River (Southern France). Journal of Hydrology, 376(3-4), 456-462.

Bailly-Comte, V., Borrell-Estupina, V., Jourde, H., & Pistre, S. (2012). A conceptual semidistributed model of the Coulazou River as a tool for assessing surface water–karst groundwater interactions during flood in Mediterranean ephemeral rivers. Water Resources Research, 48(9).

Benedicto, A., Séguret, M., & Labaume, P. (1999). Interaction between faulting, drainage and sedimentation in extensional hanging-wall syncline basins: Example of the Oligocene Matelles basin (Gulf of Lion rifted margin, SE France). Geological Society, London, Special Publications, 156(1), 81-108.

Bittner, D., Narany, T. S., Kohl, B., Disse, M., & Chiogna, G. (2018). Modeling the hydrological impact of land use change in a dolomite-dominated karst system. *Journal of Hydrology*, *567*, 267-279.

Bittner, D., Parente, M. T., Mattis, S., Wohlmuth, B., & Chiogna, G. (2020). Identifying relevant hydrological and catchment properties in active subspaces: An inference study of a lumped karst aquifer model. *Advances in Water Resources*, *135*, 103472.

Bonacci, O., Ljubenkov, I., & Roje-Bonacci, T. (2006). Karst flash floods: an example from the Dinaric karst (Croatia). Natural Hazards and Earth System Sciences, 6(2), 195-203.

Carrera, J., Alcolea, A., Medina, A., Hidalgo, J., & Slooten, L. J. (2005). Inverse problem in hydrogeology. Hydrogeology journal, 13(1), 206-222.

Chang, Y., Hartmann, A., Liu, L., Jiang, G., & Wu, J. (2021). Identifying more realistic model structures by electrical conductivity observations of the karst spring. *Water Resources Research*, *57*(4), e2020WR028587.

Clauzon, G., Suc, J. P., Popescu, S. M., Marunteanu, M., Rubino, J. L., Marinescu, F., & Melinte, M. C. (2005). Influence of Mediterranean sea-level changes on the Dacic Basin (Eastern Paratethys) during the late Neogene: the Mediterranean Lago Mare facies deciphered. Basin Research, 17(3), 437-462.

Cousquer, Y., Pryet, A., Flipo, N., Delbart, C., & Dupuy, A. (2017). Estimating river conductance from prior information to improve surface-subsurface model calibration. Groundwater, 55(3), 408-418.

Cousquer, Y., Pryet, A., Atteia, O., Ferré, T. P., Delbart, C., Valois, R., & Dupuy, A. (2018). Developing a particle tracking surrogate model to improve inversion of ground water–Surface water models. Journal of hydrology, 558, 356-365.

Cousquer, Y., Pryet, A., Delbart, C., Valois, R., & Dupuy, A. (2019). Adaptive optimization of a vulnerable well field. Hydrogeology Journal, 27(5), 1673-1681.

Darras, T., Kong-A-Siou, L., Vayssade, B., Johannet, A., & Pistre, S. (2017). Karst flash flood forecasting using recurrent and non-recurrent artificial neural network models: the case of the Lez Basin (southern France). In EuroKarst 2016, Neuchâtel (pp. 169-177). Springer, Cham.

Dausse, A., Léonardi, V., & Jourde, H. (2019). Hydraulic characterization and identification of flow-bearing structures based on multi-scale investigations applied to the Lez karst aquifer. Journal of Hydrology: Regional Studies, 26, 100627.

Drogue, C., 1964. Étude hydrogéologique des principales ressources de la région Nord Montpelliérain. Mémoire C.E.R.H. t. 1. U.S.T.L p. 62. 121.

Dubois, E., Doummar, J., Pistre, S., & Larocque, M. (2020). Calibration of a lumped karst system model and application to the Qachqouch karst spring (Lebanon) under climate change conditions. *Hydrology and Earth System Sciences*, *24*(9), 4275-4290.

Ebel, B. A., Mirus, B. B., Heppner, C. S., VanderKwaak, J. E., & Loague, K. (2009). First-order exchange coefficient coupling for simulating surface water–groundwater interactions: Parameter sensitivity and consistency with a physics-based approach. Hydrological Processes: An International Journal, 23(13), 1949-1959.

Fleckenstein, J. H., Krause, S., Hannah, D. M., & Boano, F. (2010). Groundwater-surface water interactions: New methods and models to improve understanding of processes and dynamics. Advances in Water Resources, 33(11), 1291-1295.

Fleury, P., Ladouche, B., Conroux, Y., Jourde, H., & Dörfliger, N. (2009). Modelling the hydrologic functions of a karst aquifer under active water management–the Lez spring. Journal of Hydrology, 365(3-4), 235-243.

Glaser, C., Schwientek, M., Junginger, T., Gilfedder, B. S., Frei, S., Werneburg, M., Zwiener, C., Zarfl, C. (2020). Comparison of environmental tracers including organic micropollutants as groundwater exfiltration indicators into a small river of a karstic catchment. Hydrological Processes, 34(24), 4712-4726.

Gobble, M. (2020) Identifying the Tipping Point, Research-Technology Management, 63:1, 62-67, DOI: 10.1080/08956308.2020.1686276 Drogue, C., 1964. Étude hydrogéologique des principales ressources de la région Nord Montpelliérain. Mémoire C.E.R.H. t. 1. U.S.T.L p. 62. 121.

Guilbot, A. (1975). Modélisation des écoulement d'un aquifère karstique (liaisons pluie-debit), application aux bassins de Saugras et du Lez [Modeling of flow in a karst aquifer (rainfall-discharge relations), application to Saugras and Lez basins]. Université des Sciences et Techniques du Languedoc.

Hartmann, A., Goldscheider, N., Wagener, T., Lange, J., & Weiler, M. (2014). Karst water resources in a changing world: Review of hydrological modeling approaches. Reviews of Geophysics, 52(3), 218-242.

Hartmann, A., Barberá, J. A., & Andreo, B. (2017). On the value of water quality data and informative flow states in karst modelling. *Hydrology and Earth System Sciences*, *21*(12), 5971-5985.

Hunt, R. J., Strand, M., & Walker, J. F. (2006). Measuring groundwater–surface water interaction and its effect on wetland stream benthic productivity, Trout Lake watershed, northern Wisconsin, USA. Journal of Hydrology, 320(3-4), 370-384.

Jourde, H., Batiot-Guilhe, C., Bailly-Comte, V., Bicalho, C., Blanc, M., Borrell, V., ... & Van-Exter, S. (2011). The MEDYCYSS observatory, a multi scale observatory of flood dynamics and hydrodynamics in karst (Mediterranean border Southern France). In Advances in the Research of Aquatic Environment (pp. 551-560). Springer, Berlin, Heidelberg.

Jourde, H., Lafare, A., Mazzilli, N., Belaud, G., Neppel, L., Dörfliger, N., & Cernesson, F. (2014). Flash flood mitigation as a positive consequence of anthropogenic forcing on the groundwater resource in a karst catchment. Environmental earth sciences, 71(2), 573-58

Jourde, H., Roesch, A., Guinot, V., & Bailly-Comte, V. (2007). Dynamics and contribution of karst groundwater to surface flow during Mediterranean flood. Environmental Geology, 51(5), 725-730.

Labat, D., Ababou, R., & Mangin, A. (1999). Analyse en ondelettes en hydrologie karstique. 2e partie: analyse en ondelettes croisée pluie-débit. Comptes Rendus de l'Académie des Sciences-Series IIA-Earth and Planetary Science, 329(12), 881-887.

Ladouche, B., Marechal, J. C., & Dorfliger, N. (2014). Semi-distributed lumped model of a karst system under active management. Journal of Hydrology, 509, 215-230.

Leonardi, V., Tissier, G., & Jourde, H. (2011, September). Elements de genèse des karsts péri-méditerranéens: impact de la tectonique sur l'évolution des drains karstiques (Karst Nord-Montpelliérains). In 9th Conference on Limestone Hydrogeology (pp. p-293).

Limousin, J. M., Rambal, S., Ourcival, J. M., Rocheteau, A., Joffre, R., & Rodriguez-Cortina, R. (2009). Long-term transpiration change with rainfall decline in a Mediterranean Quercus ilex forest. Global Change Biology, 15(9), 2163-2175.

Long, A. J., & Derickson, R. G. (1999). Linear systems analysis in a karst aquifer. Journal of Hydrology, 219(3-4), 206-217.

López-Chicano, M., Calvache, M. L., Martın-Rosales, W., & Gisbert, J. (2002). Conditioning factors in flooding of karstic poljes—the case of the Zafarraya polje (South Spain). Catena, 49(4), 331-352.

Maréchal, J. C., Ladouche, B., & Caballero, Y. (2018, July). Modeling the global change impacts on the Lez karst aquifer. In Eurokarst 2018.

Mazzilli, N. (2011). Sensibilité et incertitude de modélisation sur les bassins méditerranéens à forte composante karstique (Doctoral dissertation, Montpellier 2).

Mazzilli, N., Guinot, V., Jourde, H., Lecoq, N., Labat, D., Arfib, B., ... & Bertin, D. (2019). KarstMod: a modelling platform for rainfall-discharge analysis and modelling dedicated to karst systems. Environmental Modelling & Software, 122, 103927.

Moussu, F., Oudin, L., Plagnes, V., Mangin, A., & Bendjoudi, H. (2011). A multi-objective calibration framework for rainfall–discharge models applied to karst systems. *Journal of Hydrology*, *400*(3-4), 364-376.

Najib, K., Jourde, H., & Pistre, S. (2008). A methodology for extreme groundwater surge predetermination in carbonate aquifers: Groundwater flood frequency analysis. Journal of Hydrology, 352(1-2), 1-15.

Naughton, O., Johnston, P. M., & Gill, L. W. (2012). Groundwater flooding in Irish karst: the hydrological characterisation of ephemeral lakes (turloughs). Journal of Hydrology, 470, 82-97.

Olioso, A., Ollivier, C., Martin, N., Simioni, G., Weiss, M., Guillevic, P. C., ... & Huard, F. (2019, May). Monitoring Vegetation Fraction Cover of French Mediterranean Forests for Evapotranspiration and Water Stress Mapping. In ESA Living Planet Symposium 2019 (p. np).

Pinault, J. L., Amraoui, N., & Golaz, C. (2005). Groundwater-induced flooding in macropore-dominated hydrological system in the context of climate changes. *Water Resources Research*, *41*(5).

Quiers, M., Batiot-Guilhe, C., Bicalho, C. C., Perrette, Y., Seidel, J. L., & Van Exter, S. (2014). Characterisation of rapid infiltration flows and vulnerability in a karst aquifer using a decomposed fluorescence signal of dissolved organic matter. Environmental earth sciences, 71(2), 553-561.

Saltelli, A. (2002). Sensitivity analysis for importance assessment. Risk analysis, 22(3), 579-590.

Saltelli, A., Tarantola, S., Campolongo, F., & Ratto, M. (2004). Sensitivity analysis in practice: a guide to assessing scientific models (Vol. 1). New York: Wiley.

Séranne, M., Benedicto, A., Labaum, P., Truffert, C., & Pascal, G. (1995). Structural style and evolution of the Gulf of Lion Oligo-Miocene rifting: Role of the Pyrenean orogeny. Marine and Petroleum geology, 12(8), 809-820.

Sivelle, V., Jourde, H., Bittner, D., Mazzilli, N., & Tramblay, Y. (2021). Assessment of the relative impacts of climate changes and anthropogenic forcing on spring discharge of a Mediterranean karst system. Journal of Hydrology, 126396.

Sobol, I. M. (2001). Global sensitivity indices for nonlinear mathematical models and their Monte Carlo estimates. Mathematics and computers in simulation, 55(1-3), 271-280.

Sophocleous, M. (2002). Interactions between groundwater and surface water: the state of the science. Hydrogeology journal, 10(1), 52-67.

Teixeira Parente, M., Bittner, D., Mattis, S. A., Chiogna, G., & Wohlmuth, B. (2019). Bayesian calibration and sensitivity analysis for a karst aquifer model using active subspaces. *Water Resources Research*, *55*(8), 7086-7107.

Thiery D, Bérard P, Camus A (1983) Captage de la source du Lez. Etude de la relation entre la source et son réservoir aquifère. Rapport public BRGM/83-SGN-167-LRO. BRGM

Vallejos, A., Andreu, J. M., Sola, F., & Pulido-Bosch, A. (2015). The anthropogenic impact on Mediterranean karst aquifers: cases of some Spanish aquifers. *Environmental Earth Sciences*, *74*(1), 185-198.

Winter, T. C. (1999). Relation of streams, lakes, and wetlands to groundwater flow systems. Hydrogeology Journal, 7(1), 28-45.

Zhou, H., Gómez-Hernández, J. J., & Li, L. (2014). Inverse methods in hydrogeology: Evolution and recent trends. Advances in Water Resources, 63, 22-37.

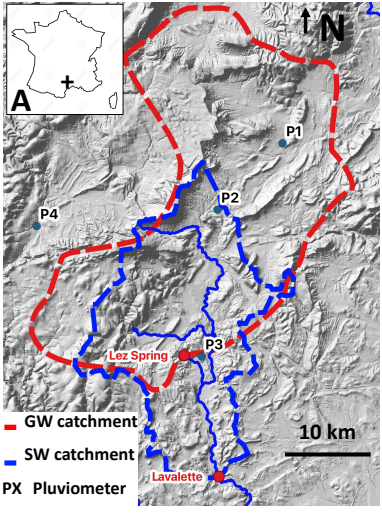
A
N
P1
P2
P4
P3
Lez Spring
Lavalette
10 km
GW catchment
SW catchment
PX Pluviometer

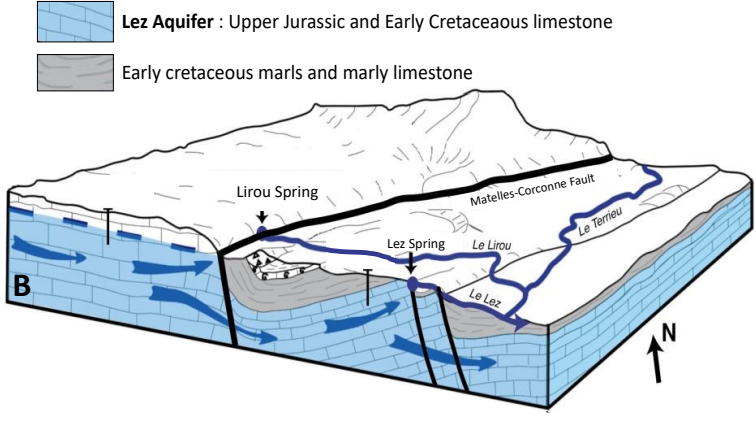
Lez Aquifer : Upper Jurassic and Early Cretaceaous limestone
Early cretaceous marls and marly limestone
Lirou Spring
Matelles-Corconne Fault
Le Terrieu
Lez Spring
Le Lirou
Le Lez
B
N

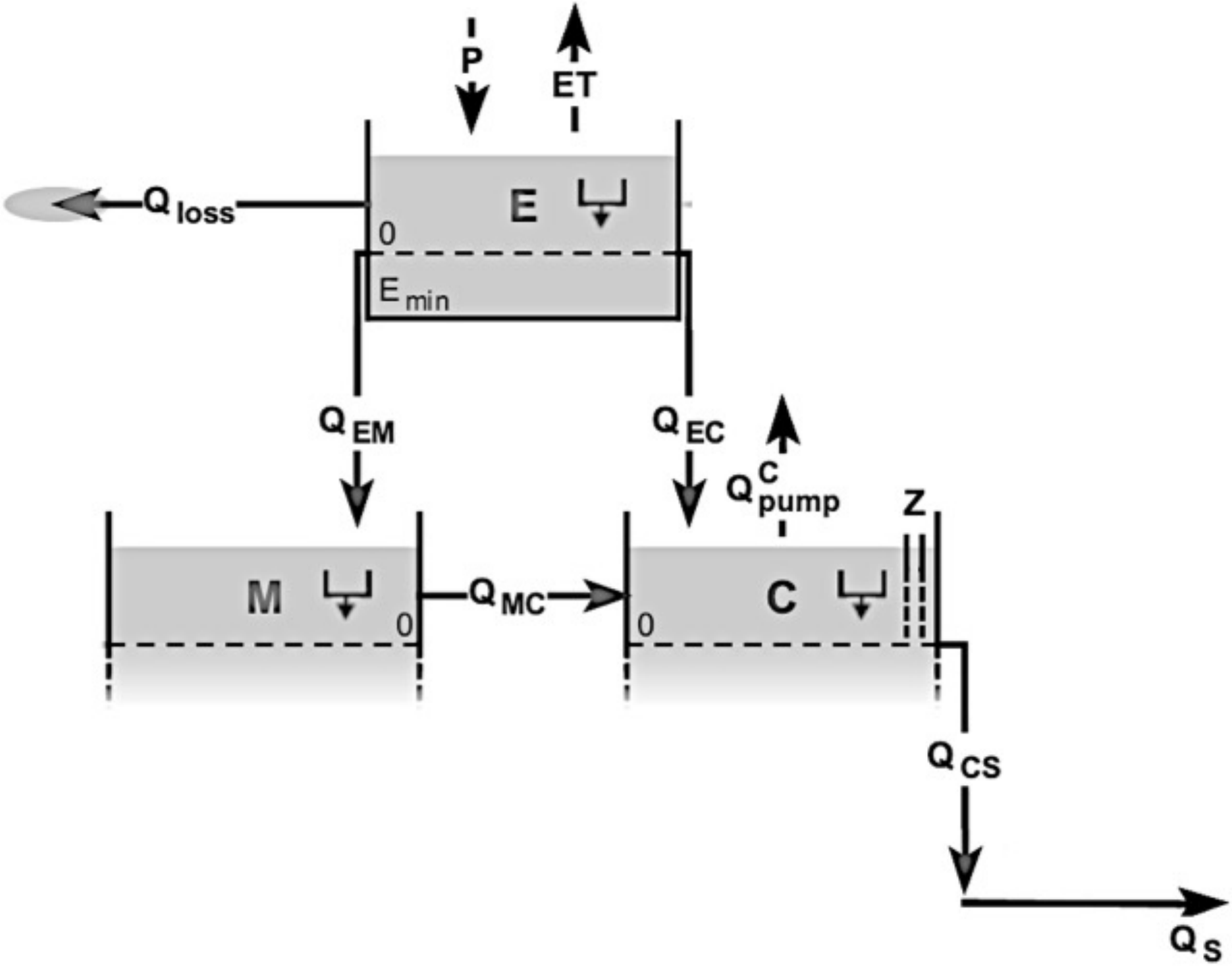
P
ET
Q loss
E
0
E min
Q EM
Q EC
Q C pump
Z
M
Q MC
C
0
0
Q CS
Q S

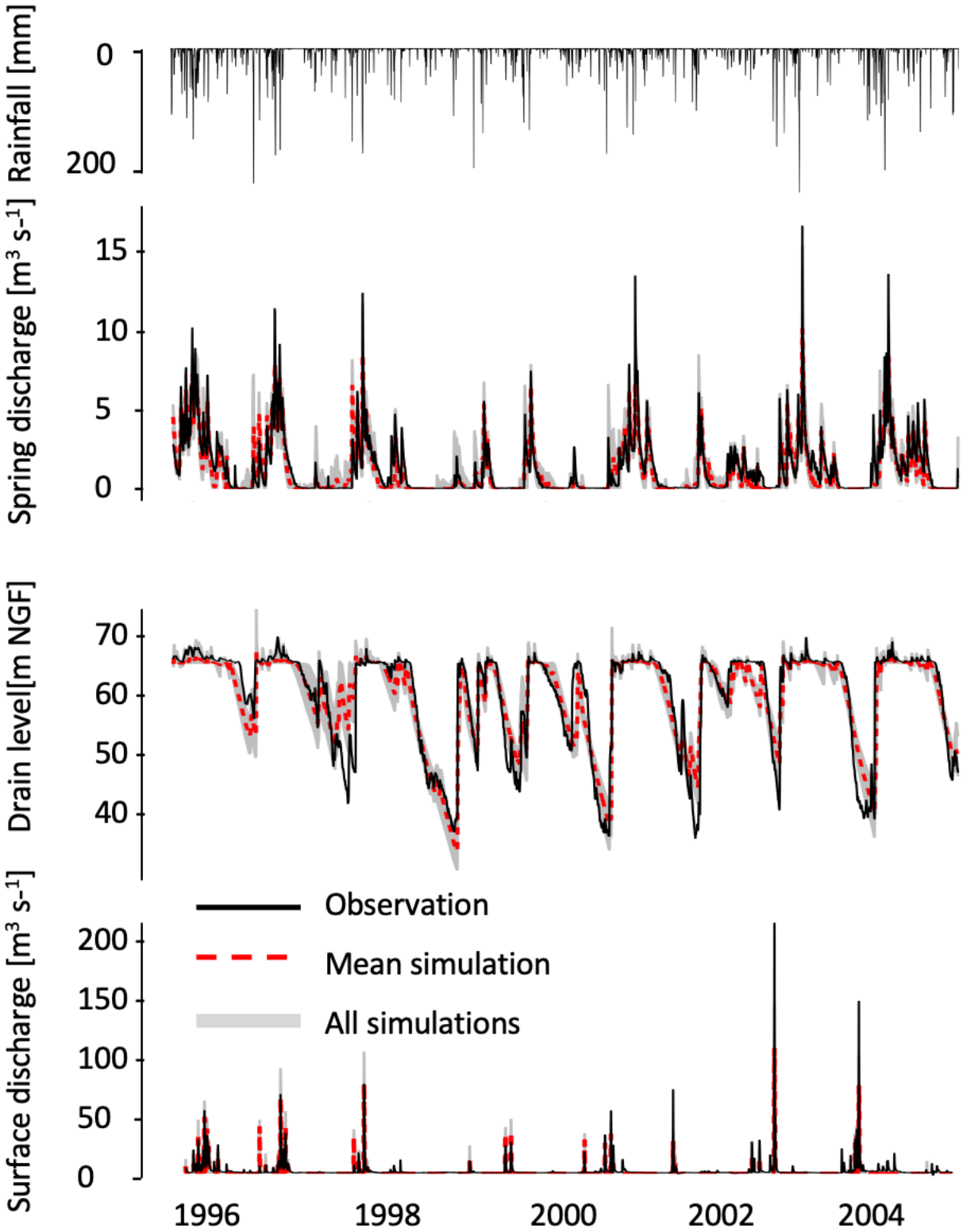
Rainfall [mm]
0
200
Spring discharge [m³ s-1]
15
10
5
0
Drain level[m NGF]
70
60
50
40
Surface discharge [m³ s-1]
200
150
100
50
0
Observation
Mean simulation
All simulations
1996
1998
2000
2002
2004

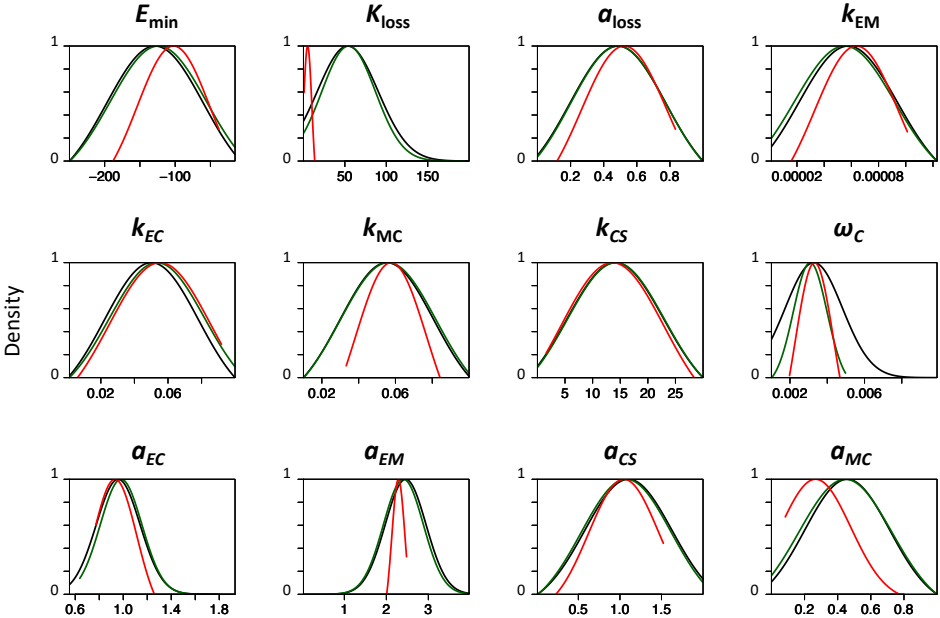

$\phi tot = \phi Q_{GW}$ $\phi tot = 0.5\,\phi Q_{GW} + 0.5\,\phi_Z$ $\phi tot = \frac{1}{3}\,\phi Q_{GW} + \frac{1}{3}\,\phi_Z + \frac{1}{3}\,\phi Q_{SW}$

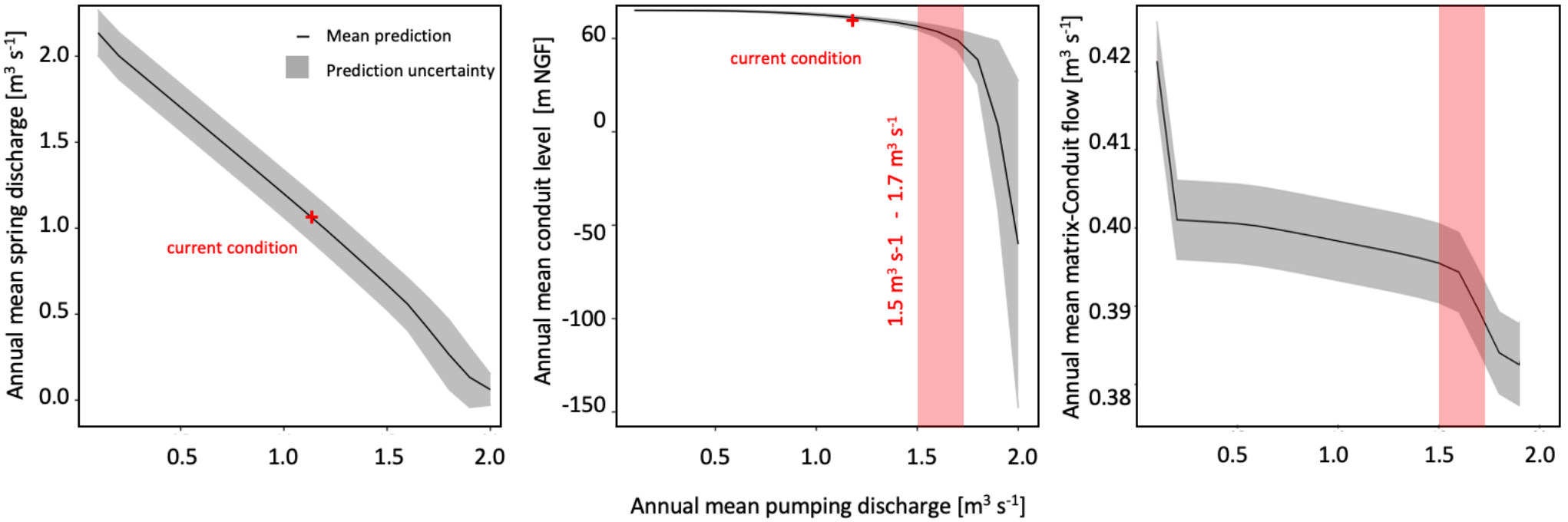
Mean prediction
Prediction uncertainty
current condition
Annual mean spring discharge [m³ s⁻¹]
2.0
1.5
1.0
0.5
0.0
0.5
1.0
1.5
2.0
current condition
1.5 m³ s-1 - 1.7 m³ s-1
Annual mean conduit level [m NGF]
60
0
-50
-100
-150
0.5
1.0
1.5
2.0
Annual mean matrix-Conduit flow [m³ s⁻¹]
0.42
0.41
0.40
0.39
0.38
0.5
1.0
1.5
2.0
Annual mean pumping discharge [m³ s⁻¹]

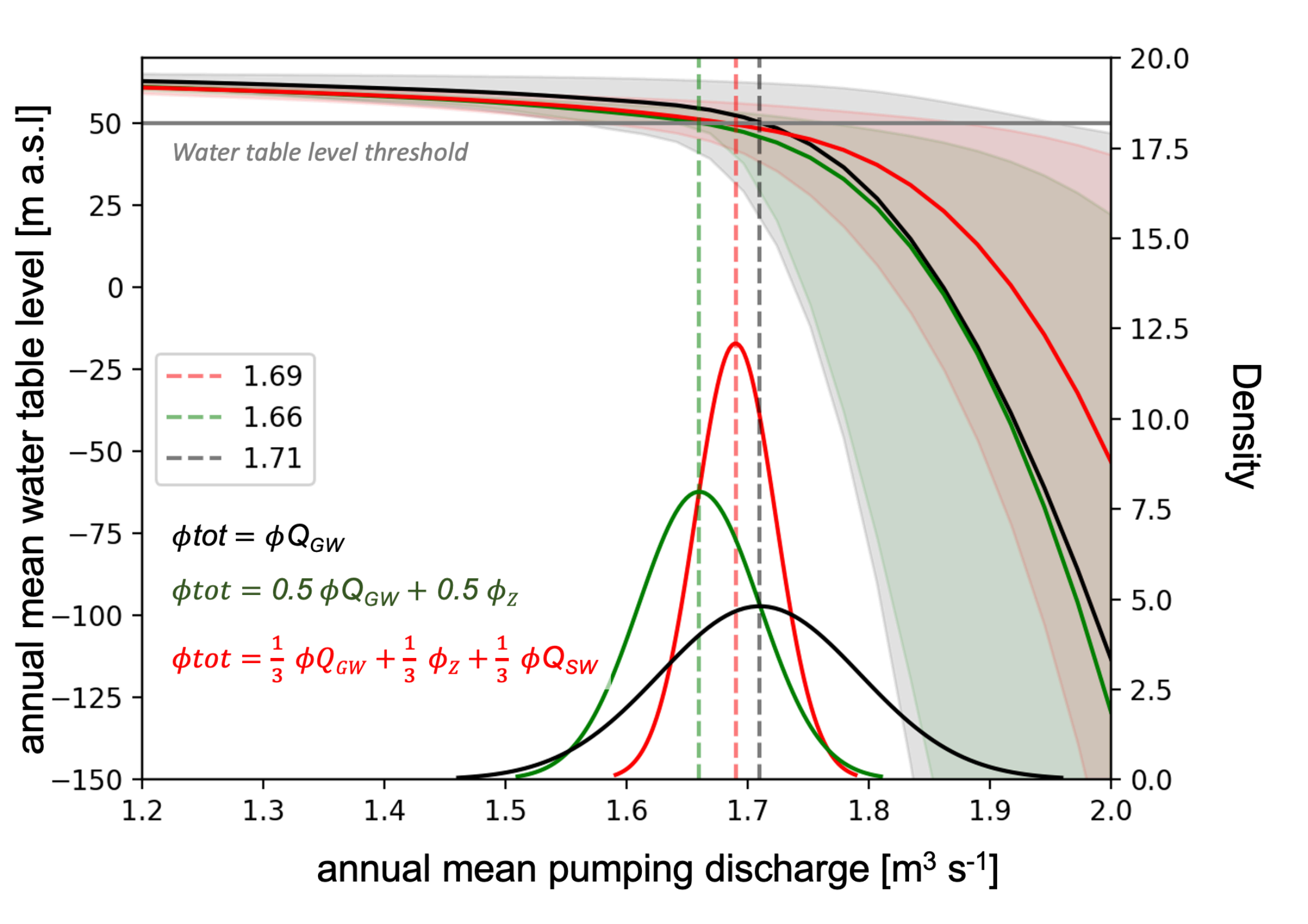
annual mean water table level [m a.s.l]
annual mean pumping discharge [m³ s⁻¹]
Density
Water table level threshold
1.69
1.66
1.71
ϕtot = ϕQ_GW
ϕtot = 0.5 ϕQ_GW + 0.5 ϕ_Z
ϕtot = 1/3 ϕQ_GW + 1/3 ϕ_Z + 1/3 ϕQ_SW
50
25
0
−25
−50
−75
−100
−125
−150
20.0
17.5
15.0
12.5
10.0
7.5
5.0
2.5
0.0
1.2
1.3
1.4
1.5
1.6
1.7
1.8
1.9
2.0

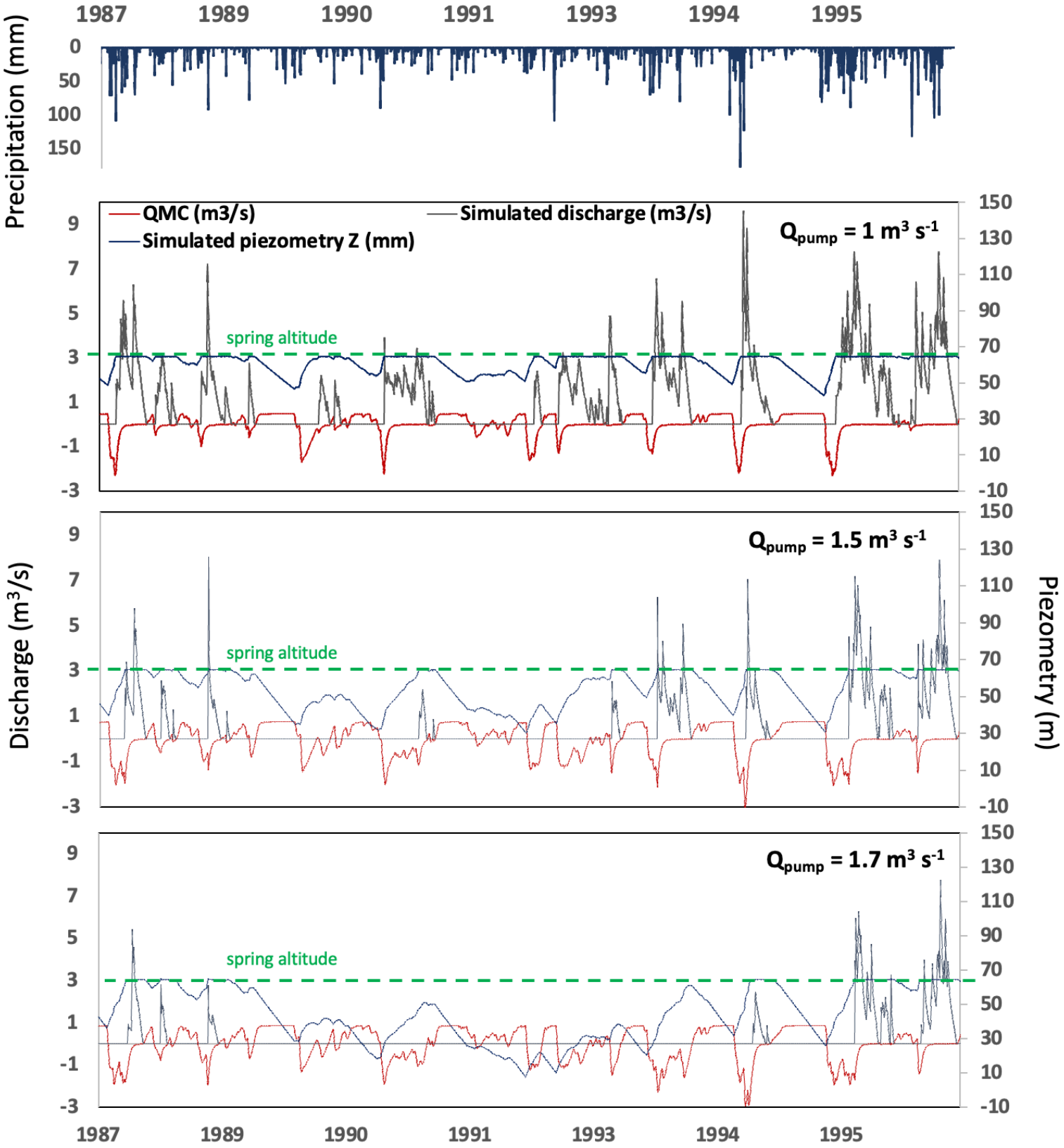
Precipitation (mm)
1987
1989
1990
1991
1993
1994
1995
0
50
100
150
QMC (m3/s)
Simulated discharge (m3/s)
Simulated piezometry Z (mm)
Qpump = 1 m3 s-1
spring altitude
Qpump = 1.5 m3 s-1
spring altitude
Qpump = 1.7 m3 s-1
spring altitude
Discharge (m3/s)
Piezometry (m)
9
7
5
3
1
-1
-3
150
130
110
90
70
50
30
10
-10

Parameter	Lower bound	Upper bound	Unit	Description
E_{min}	-250	-15	m	minimum water level in compartment E
k_{loss}	0	100	m s^{-1}	specific discharge coefficient for the Qloss discharge law
E_{loss}	50	150	m	threshold for the activation of the Qloss discharge law
k_{EM}	1.23E-06	1.23E-04	m s^{-1}	specific discharge coefficient for discharge law from E to M
k_{EC}	0.001	0.1	m s^{-1}	specific discharge coefficient for discharge law from E to C
k_{CS}	0	30	m s^{-1}	specific discharge coefficient for discharge law from C to S
k_{MC}	0.01	0.1	m s^{-1}	specific discharge coefficient for discharge law from M to C
ω_c	0.001	0.005	-	effective porosity
a_{EC}	0.5	1.5	-	exponent of the discharge law from E to C
a_{MC}	0	1	-	exponent of the discharge law from M to C
a_{EM}	2	4	-	exponent of the discharge law from E to M
a_{CS}	0	2	-	exponent of the discharge law from C to S
Z_0	fixed : 65		m	overflow threshold elevation of the E compartment
R_A	fixed : 154 1E6		m^2	recharge area
M_0	fixed : -22		m	overflow threshold elevation of the M compartment
C_0	fixed : 15		m	overflow threshold elevation of the C_0 compartment

Obs. considered in Φtot	Nb. Sim. with Φtot > 0.6	best Φtot- Calibration period	best Φtot - Validation 1	best Φtot - Validation 2
1) Q_{GW}	6424	0.8	0.72	0.77
2) Q_{GW} + Z	2632	0.73	0.6	0.59
3) Q_{GW} + Z + Q_{SW}	52	0.64	0.58	0.56